Multidiszciplináris Tudományok, 15. kötet, 2. sz. (2025) pp. 31–49. **https://doi.org/10.35925/j.multi.2025.2.3**

INVESTIGATION OF THE TIME-HISTORY OF THE COVID-19 PANDEMIC IN HUNGARY BY SIGMOID CURVES – COMPARISON OF SEVERAL WAVES

Ferenc János Szabó
associate professor, Institute of Machine-and Product Design,
University of Miskolc, Hungary, 3515 Miskolc-Egyetemváros, e-mail: ferenc.szabo@uni-miskolc.hu

Abstract
Sigmoid curves are multidisciplinary curves, because they are used in many fields of life (economy, statistics, engineering, product design, iteration history curves of optimization algorithms, environmental science, health sciences, etc.) for the investigation and prediction of many phenomena. In this paper the history of COVID-19 infection in Hungary from March 2020 until June 2023 is investigated by sigmoid curves. Since the pandemic had several waves, by analysing the sigmoid curves of each waves it is possible to compare their characteristics. This comparison can lead to interesting new conclusions, for example it is possible to define the "mutation delay" and the comparison of this delay of several waves can show the effect of vaccination. Comparing the derivatives and integrals of the sigmoid curves, more conclusions can be drawn. In the days when this paper is written, the relevance of these investigations and comparisons may increase again, because of new and aggressive COVID variants, BA.5 or JN.1. In case of appropriate data, it would be possible to compare the curves of these variants and other waves, which could give useful information about intensity, aggressivity, or mortality of the waves.

Keywords: *COVID-19 in Hungary, Sigmoid curves, History of the desease from 2020 until 2023.*

1. Introduction

The application of sigmoid curves makes it easy to understand and forecast the investigated phenomenon. They can be used in many fields of our life, because these curves are highly interdisciplinary curves:

The first application of the sigmoid curves was in biology by (Malthus, 1798), who investigated the possible number of particles in several populations, in case of a non limited or unconstrained reproduction process. For limited or constrained reproduction (Verhulst, 1847) described the growing process by a special sigmoid curve, by logistic curve. (Pearl and Reed, 1920) applied the logistic curve for the prediction of the population of the USA. (Bertalanffy, 1960) defined a special type of sigmoid function (the growth function), for the study of the growth of shark fins. This type of curve shows a not very typical saturation part, but is very efficient in the description of the growth process. This type of growth function can be applied successfully in agriculture to describe the growth of several species of animals or plants in stock-raising or cultivation. (Richards, 1959) and (Kozusko et al., 2003) applied this type of growth function in medical science for the investigation of the growth of tumours. (Moore, 1965) described the increase of the capacity of electronic devices as a function of time by using logistic curves.

To cite further examples from a variety of disciplines, (Mansfield, 1961) applied the sigmoid curves in product development, innovation management and market analysis. (Jang et al., 2005) investigated the history of the mobile phone market in several countries of the world. Pulsating and/or multiwave phenomena were shown by (Meyer, 1994) using multilogistic curves. (Nikosz, 2009) applied the sigmoid curves for social phenomena, showing interesting historical examples. (Gruener, 2024) performed a survey in Germany to rate the reliability of several opinions from several fields of our life, including COVID-19.

(Szabó, 2011, 2017, 2018, 2019, 2020, 2021) has published a number of papers on applications of sigmoid curves in different fields of life: the history of world sport records (2011), comparison and qualification system for results and achievements of groups (EBSYQ, Evolutionary Based System for Qualification of Group Achievements, 2017), comparison and setting of optimization algorithms (2018), investigation and prediction of the plastic-contamination of seas and oceans of the Earth (2019), analysis of the wear curves of manufacturing tools (2020) and use of sigmoid curves in product design in the investigation of product life-curves (2021). Rézsóné (2020) applied sigmoid curves for the comparison of student groups writing the same exam.

The sigmoid curves have been used to describe the time history of several diseases: (Dénes et al., 2019) created a mathematical model describing the Zika virus and they applied the model later for COVID-19. They used a curve having a shape similar to the derivative of the logistic curve. Several authors are using sigmoid curves for investigation of SARS-COVID-2 disease in the world. (Kapoor, 2022) studied the pandemic response in India, comparing sociodemographic risk factors. (Lennert, 2021) modelled the first wave of the pandemic in Hungary. The (CDC COVID-19 Response Team, 2020) reported severe outcomes among COVID-19 in the USA. (Du et al., 2020) studied the serial interval of COVID-19 among publicly reported confirmed cases in China. (Shen, 2020) carried out logistic growth modelling of COVID-19 proliferation in China and its international implications. (Konstantinov, 2021) used sigmoid models for the COVID-19 pandemic and results were in good agreement with official data in Europe. (Novoa-Munoz, 2022) used sigmoid models to predict the number of infected cases and deaths of COVID-19 in Chile. (Anilkumar, Srividya and Sowjanya, 2023) performed COVID-19 classification using a sigmoid based hyper parameter and they predicted the virus in CT and MR images.

Since the pandemic had several waves, authors followed the growth of the disease by using sigmoid curves of two and more waves. (Somefun, Akingbade and Dahunsi, 2020) modelled the pandemic growth by n-logistic sigmoid curves, with a high degree of accuracy. (Szabó, 2022) analysed the time-history of the pandemic in Hungary with multiwave sigmoid curves and compared two waves on the basis of the parameters of their sigmoid curves and equations. (Dubey, Mishra and Goswami, 2022) modelled and predicted the spread of COVID-19 by using mathematical modelling with the Atangara Baleanu fractional derivative. (Somathilake, 2022) made a mathematical model for control strategies against the pandemic. (Al-Rahman, Hussien and Yehia, 2023) performed a double-sigmoid analysis of the disease in Egypt. (Mousa, 2023) also proposed double sigmoid growth curves for the modelling and estimation of the COVID-19 disease.

In this paper the time history of the COVID-19 in Hungary is shown and it is analysed with multiwave sigmoid curves and their derivatives. Comparison is shown for several waves of the disease, on the basis of the comparison of several parameters of the curves and of their derivatives.

2. Approximation with sigmoid curves

In *Table 1* several sigmoid curves can be found, but it can be discovered easily from the table that two important types of sigmoid curves can be identified: the growth-type curve (used by Törnquist, Mitscherlich and Bertalanffy), having a growth stage and saturation stage, and the logistic type sigmoid curve (Pearl and Reed), which has these two stages and in addition has an exponential growth stage in the beginning. The third form of the sigmoid curves can be the Lorentz function, but in this case not the curve itself will hold the sigmoid shape but its integral.

For further investigations two very typical types of sigmoid curves will be used: the Bertalanffy curve is selected as a growth curve and the Pearl and Reed curve is used as logistic curve. Thus it will always be easy to decide which type the investigated phenomenon is (pure growth or logistic) and the comparison and qualification work after the approximation can be done for the type giving the better regression coefficient.

The equations of the two selected curves:

Pearl and Reed (logistic) curve:

equation of the curve: $y(x) = \frac{K}{1+ce^{-rx}}$, first derivative: $\frac{dy(x)}{dx} = \frac{Kcre^{-rx}}{(1+ce^{-rx})^2}$, integral:

$$\int y(x)dx = -\frac{K}{r}\ln(e^{-rx}) + \frac{K}{r}\ln(1+ce^{-rx}) \tag{1}$$

Bertalanffy (growth) curve:

equation of the curve: $y(x) = K(1 - ce^{-rx})$, first derivative: $\frac{dy(x)}{dx} = Krce^{-rx}$, integral:

$$\int y(x)dx = Kx + \frac{Kc}{r}e^{-rx} \tag{2}$$

For the approximation of the real data by sigmoid curves, the method of least squares is used. During the investigations, the data describing the given phenomenon are available in sets of discrete values. These data will be approximated by sigmoid curves, determining the parameter values of *K, r, c* which give the best approximation. After the approximation process, when we know the effects of these parameters on the shape and behaviour of the curves, it is possible to start the comparison and evaluation process. This can be the basis of an objective and detailed evaluation and comparison process. When using the method of least squares it is necessary to approach the given discrete values (x_i, y_i), i = 1, 2, 3, … , n, by a function $y^* = f(x)$, while the parameters of the curve should give the minimum possible value of the sum of the squares of the differences. This means that regarding the approximating function values $f(x_i) = y^*_i$, we have to find:

$$H = \sum_{i=1}^{n}(y_i - y_i^*)^2 = min \ . \tag{3}$$

The minimum is possible if the first derivative of the function *H* is 0, therefore:
$\frac{\partial H}{\partial K} = 0$, $\frac{\partial H}{\partial r} = 0$, $\frac{\partial H}{\partial c} = 0$, giving three equations for the three unknowns *K*, *r* and *c*, so it is possible to find the parameters for the best approximation. Another possible way to find the minimum of *H* as a function of the three parameters, is to solve the problem as an unconstrained minimisation task of *H* using the three parameters as design variables. In this paper this method of optimisation is selected for the calculation of the best curve-parameters during the approximations. In this paper for the numerical

solution of this optimisation task the Nelder–Mead "simplex" algorithm (1965) is used. For the two selected curves it is important to determine, which curve gives the best approximation for the discrete data, because this is the base of the classification of the conclusions: the better the approximation quality, the stronger the derived conclusion is. Thus, it is necessary to calculate the regression coefficient for both of the curves. Since the two selected curves are non-linear, before the analysis of the regression it is necessary to transform the equations of the curves into linear form. The regression coefficient calculated for these resulting linear functions will show which curve has the better correlation with the discrete data, so the conclusions derived from that curve will be stronger, i.e. more realistic for the given group. The value of the regression coefficient is always between –1 and +1. If it has a value of 0, that means there is no relationship between the curve and the discrete values. The closer the absolute value of the regression coefficient to 1, the better the correlation between the data and the approximation curve.

If the regression coefficient is negative, it shows a decreasing tendency, while positive value shows an increase. This means that the conclusions derived from a curve having weak regression coefficient will be not true, strong or accurate enough, but the conclusions derived on the basis of a curve having good correlation will be true and adequate, or strong. For calculation of the regression coefficient, the curve equations need to be transformed into linear form for both of the selected functions. For that the Fisher–Pry transformation (1971) can be used:
Linear transformation of the Bertalanffy function:

$$y(x) = K(1 - ce^{-rx}) \ , \ ce^{-rx} = \frac{K-y(x)}{K} \ , \ ln\, c + ln\, e^{-rx} = ln\left(\frac{K-y(x)}{K}\right) \ , \tag{4}$$

therefore the linear function for the Bertalanffy-curve: $y^* = a + bx$, where $a = \ln c$, $b = -r$.
The linear transformation of the Pearl and Reed function can be done in a similar way:

$$y(x) = \frac{K}{1+ce^{-rx}} \ , \ \frac{K-y(x)}{y(x)} = ce^{-rx} \ , \ ln\, c + ln\, e^{-rx} = ln\frac{K-y(x)}{y(x)} \ , \ y^* = a + b\,x \tag{5}$$

The regression coefficient can be calculated as:

$$R_{lin} = \frac{A_{xy} - \frac{B_{xy}}{n}}{\sqrt{\left(C_x - \frac{D_x}{n}\right)\left(C_y - \frac{D_y}{n}\right)}} \tag{6}$$

where: $A_{xy} = \sum_{i=1}^{n} x_i y_i$, $B_{xy} = \sum_{i=1}^{n} x_i \sum_{i=1}^{n} y_i$, $C_x = \sum_{i=1}^{n} x_i^2$, $D_x = \left(\sum_{i=1}^{n} x_i\right)^2$
$C_y = \sum_{i=1}^{n} y_i^2$, $D_y = \left(\sum_{i=1}^{n} y_i\right)^2$.

In *equation (6)* one can calculate the linear regression coefficient of the y* transformed function determined in *equation (4)* or *(5)*, but for simplicity we returned to the y notation.

Table 1
Several types of sigmoid curves

The curve	Derivative	Integral
Törnquist I (1936)		
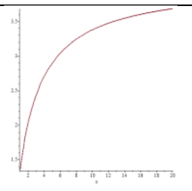	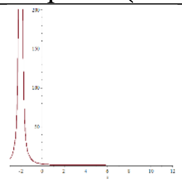	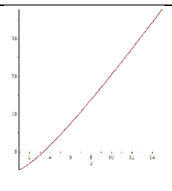
Törnquist II (1981)		
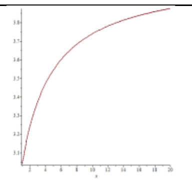	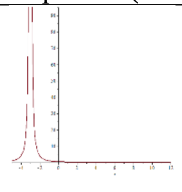	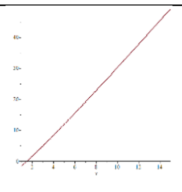
Mitscherlich (1909)		
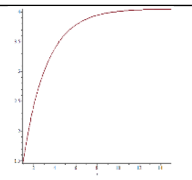	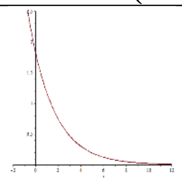	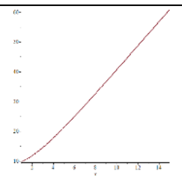
Pearl and Reed (1920)		
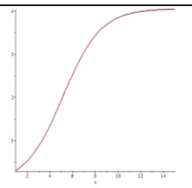	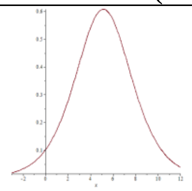	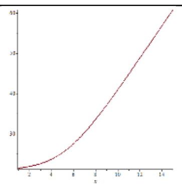
Bertalanffy (1960)		
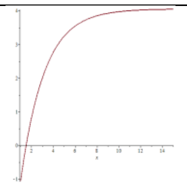	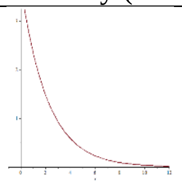	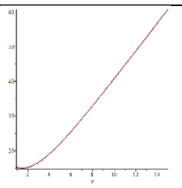
Lorentz (1905)		
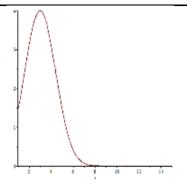	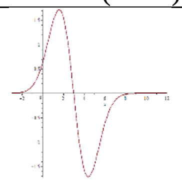	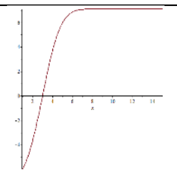

3. History of the COVID-19 disease in Hungary

The first day of this investigation is 15 of March 2020, because this was the day when the first death attributed to COVID-19 occurred in Hungary. In *Figure 1* the sigmoid curves of the number of the infections can be seen (left) and the number of the deaths (right), in function of the days elapsed. The source of the data is the COVID-19 Dashboard on the homepage of the Johns Hopkins University of Medicine (2020), which gave fresh numbers of infections and deaths for all countries of the world every day.

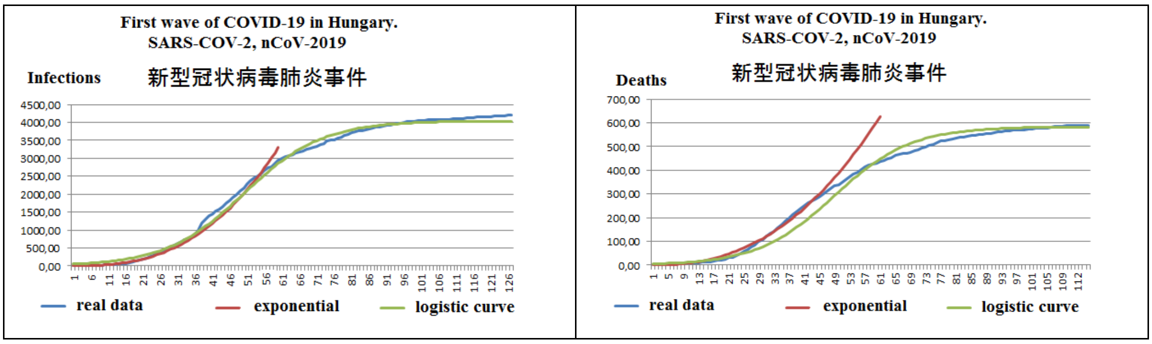

Figure 1. *The first wave of the COVID-19 in Hungary, number of infections (left) and number of deaths (right) in function of elapsed days*

Figure 1 shows that the first part of the history of the disease has exponential growth, which can increase quickly into very high numbers, if people do nothing against it. This shows that it is because of the heroic work of medical experts, decision makers and hospital workers that the situation started to become normalized approximately fifty days after the starting of the disease. The starting point of this changing is where the curve has an inflexion point: after this time the normalization will be in progress. Also, it is possible to detect the good correlation between the real data and the approximating logistic curves.

Regarding *equation (1)*, the parameters of the curves can be seen in *Table 2*.

Table 2
Parameters of the approximating sigmoid curves

Curve	K	r	c	Inflexion point (day)
Deaths	584	0.0987	124.66	43
Infections	4,043	0.0883	83.29	50

Comparing the parameters of the curves, the r parameter is higher in case of deaths than in case of infections, meaning that the growth of the numbers is quicker in case of deaths. The K parameter is higher in case of infections: this shows the maximum numbers achieved at the end of the normalization. The c parameter has a more complex effect: it can modify the maximum possible numbers achieved and also the earlier or later appearance of the inflexion point. The layout of the curves is very similar, so it could be difficult to qualify or compare the curves by eye only, but the comparison of the parameters shows even the smallest differences very accurately, making more accurate comparisons possible.

The inflexion point has an other very important role: During any prediction process or forecast building, it is very important to understand, that before the point of inflexion one can see only the exponential growth, which shows what will occur if people do nothing: the effects of protecting actions will appear only after the inflexion point. This means that we should not give predictions for the future behaviour of the disease when we are before the inflexion point, because in that time it is not known when and what kind of actions will be taken. Before the inflexion point one can give predictions only for the exponential growth, so it is possible to predict only what will be if people will do nothing. After the inflexion point, on the basis of the parameters of the curves, it will be possible to predict the possible maximum number of infections or deaths, and it will be possible to see the speed of the growth. The place of the inflexion point will show the effectiveness of the measures and activities against the disease, because an earlier inflexion point means more rapid, more effective measures, which can decrease the final maximum of the number of cases.

Figure 2 shows the approximating curve, its derivative and its integral (from left to right) as a function of the days elapsed, for the case of infections and *Figure 3* for the case of deaths.

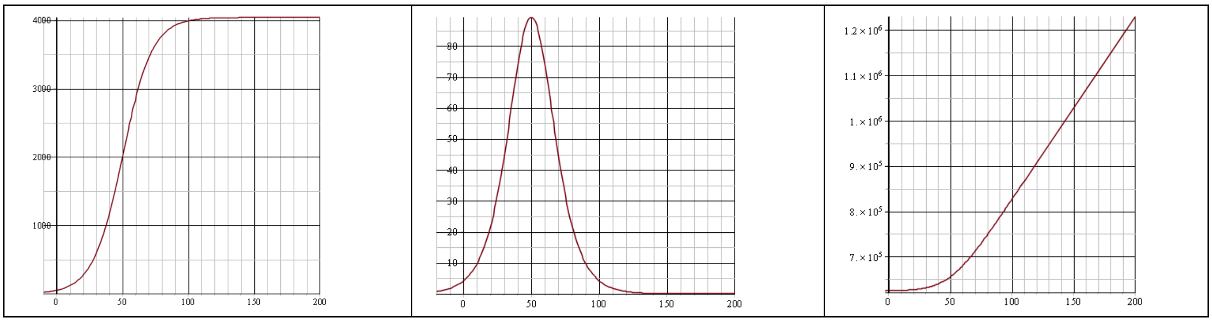

***Figure 2**. The approximating sigmoid curve, its derivative and its integral for infections*

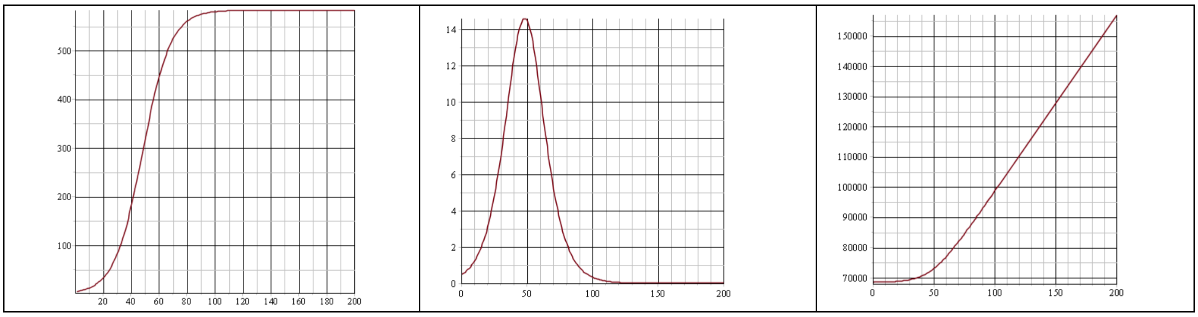

***Figure 3**. The approximating sigmoid curve, its derivative and its integral for deaths*

Equation (1) shows the equations of the curve, derivative and integral, where the parameters are the same as in *Table 2*. While the shape of the integrals of the curves is very similar, it would be interesting to compare the derivatives. In case of the "bell-shape" of the derivative curves, the place and value of the maximum is an important and easily comparable characteristic. Since the derivative is in connection with the celerity of the growth, the place of the maximum shows, how quickly the maximum of the growth occurs, so how aggressive the disease is. The value of the maximum shows the deepest point of the disease, where the maximum increase in the number of cases appears. It may be useful to compare the sharpness of the derivative curves, calculating the width of the curve at half of the maximum value. This width is in connection with the "significance" or extent of the phenomenon, higher width means more significance than lower width. For the investigation of this characteristic it could be useful to define a "significance factor", or "extent factor", which is the ratio of the width at half maximum ($w_{0.5}$) over the time of the maximum (t_m):

$$\gamma_s = \frac{t_m}{w_{0.5}} \tag{7}$$

Comparing the significance factor can tell us how strong the investigated phenomenon is, for example here it will show, whether the growth of number of deaths or infections is stronger. On the basis of this factor, later it will be possible to compare the mortality rate of the different waves. While the curves of the derivatives for deaths and for infections seem to be very similar, a comparison of this factor (see *Table 3*) shows the difference between the two curves, so it can be once more concluded that more accurate comparison is possible on the basis of the parameters of the curves than a first glance can offer.

Table 3
Characteristics of the derivatives of the approximating sigmoid curves

Curve	Place of the maximum	Value of the maximum	Width at half-maximum	Significance factor
Deaths	43	14.5	33	0.77
Infections	50	89	40	0.80

Comparison of the place of the maximum can show how quickly the measures against the disease appear. If the measures begin later, the inflexion point appears later, therefore the period of exponential growth is longer, which can cause higher numbers at the end, and a higher *K* parameter.

The integral of the approximating sigmoid curve is close to the linear shape, because this is the area under the curve. It shows the accumulated numbers of cases as a function of time. This can be useful information for experts of epidemiology for the predicting possible overstressing of hospitals or can give them useful data for the possible quantity of medicaments or devices necessary during the defence and protection activity against the pandemic.

During the summer of 2020, the first wave stabilized and the number of infections and deaths was very low. At the end of August the second wave started and in September it was already clear that the number of infections and deaths would be much higher in the second wave, than during the first wave *(Figure 4)*. The inflexion points were considerably later than in the case of the first wave, therefore much higher numbers occurred *(Figure 5)*, for both infections and deaths, so it was evident that the second wave was much worse than the first one was. The second wave of the death cases started a little bit later than the curve of infections, by approximately two weeks. This is because of the period of incubation and the deterioration of the disease in infected patients.

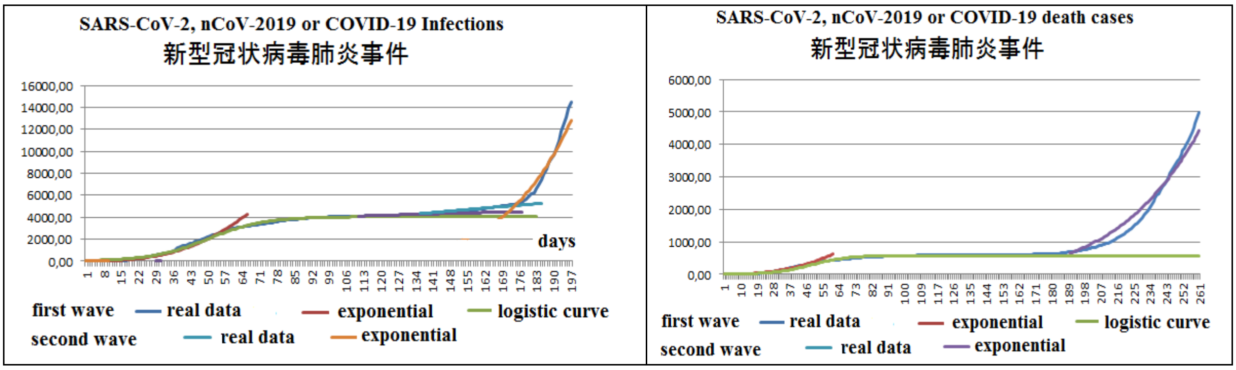

Figure 4. *The curves of the second wave*
(Infections: as of 16 September 2020, deaths: as of 1 December 2020)

In the beginning of January 2021, because of the variety of measures, and separation during the Christmas and New Year holidays, and other decisions against the disease, the inflexion points appeared and the saturation process began. This normalization period was short, because in the middle of January (after the 300th day) a new wave started with a new virus variant. This third wave was the longest and highest wave since the beginning of the disease *(Figure 5)*. In *Figure 5* it is clear that the normalisation period is considerably longer in case of the third wave than it was in case of the previous wave, this is because the new variant of the virus arrived later in the third wave and in the second wave a variant arrived much earlier. This fact also could be a good basis of comparison and it is useful to define it numerically, too, in order to see the differences more precisely. (see *Table 9*). In *Figure 5* the starting of the fourth wave can also be seen with its exponential curve.

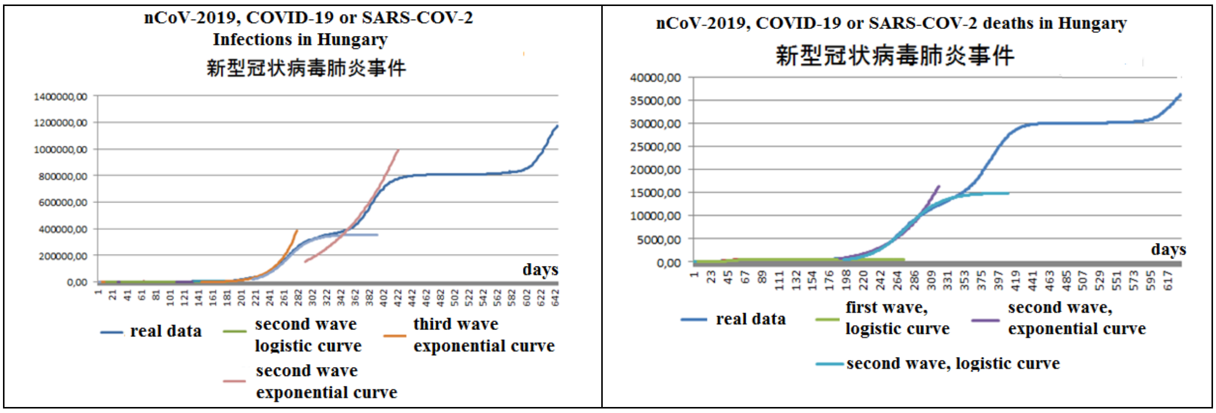

Figure 5. *The third wave* (infections and deaths curve: as of 9 December 2021)

Figure 5 shows in one diagram all four waves of the disease, which makes possible to compare for the first look the different waves. Different *K* parameters (maximum expectable number of cases), different *r* parameters (speed of growth) and different length of the normalized state (different times at which the new variant appears). In the following chapter of this paper these characteristics will be compared more accurately numerically, too.

4. Comparison of several waves of the disease

Regarding the full history curve of the COVID-19 disease in Hungary *(Figure 5)*, it is evident, that the disease has several waves, therefore its detailed description is possible only by using multilogistic curves. Each logistic curve has two parts: the first part is the free (unconstrained) growth period, which shows exponential increase of the numbers, and the second part is the saturation period (constrained growth), until the stop of the growth. It is possible to build the equations of the first part (exponential curve) and also of the second part (sigmoid curve), to compare their curves and the parameters more easy.

The first part of a wave curve is the exponential curve:

$$y = cx^r \tag{8}$$

In order to more easily compare the different waves, the exponential parts of the curves are transformed into the origin of the coordinate system (*Figure 6* for the number of infections and *Figure 7* for the number of deaths) and *Tables 4* and *5* show the parameters of the exponential equations. The comparison of the exponential curves gives information about the aggressiveness of the wave in the starting period. Both the infections and the death numbers curve show that the virus variant of the third wave was the most aggressive one at the start.

The second part of the logistic curves is the saturation:

$$y = \frac{K}{1+ce^{-rx}} \quad . \tag{9}$$

The saturation curves can be seen in *Figures 8* and *9*, (also transformed into the origin of the coordinate system) and the parameters of the curves are in *Tables 6* and *7*.

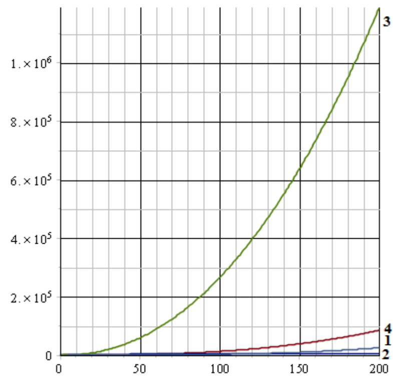

Figure 6. *Exponential curves (number of infections as a function of days)*

Table 4

Parameters of the exponential curves (infections)

Param.	Wave1	Wave2	Wave3	Wave4
c	0.0522	1596.445	5.1259	0.0010327
r	2.70	0.2001	3.262e+08	3.2139875

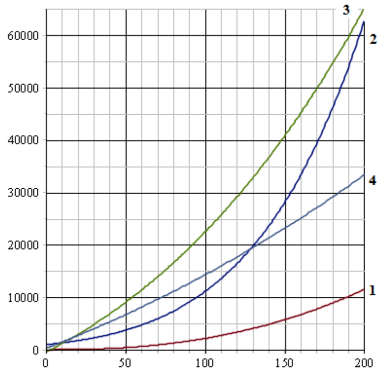

Figure 7. *Exponential curves (number of death cases as a function of days)*

Table 5

Parameters of the exponential curves(deaths)

Param.	Wave1	Wave2	Wave3	Wave4
c	0.031	1.4e-11	1.949e-06	0.000217
r	2.42	6.015	3.862	2.9331075

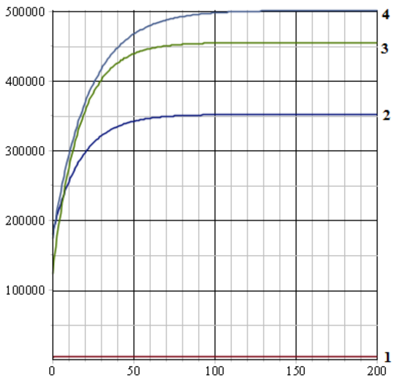

Figure 8. *Logistic curves (infections)*

Table 6

Parameters of the saturation curves(infections)

Param.	Wave1	Wave2	Wave3	Wave4
K	4043	3.56e+05	8.085e+05	1.3109e+06
c	2.4253	4.13e+06	5.385e+09	5.5330e+11
r	0.0883	0.057	0.06051379	0.04511322

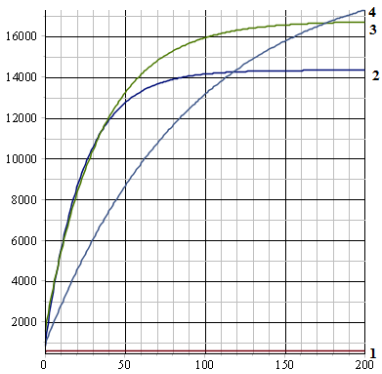

Figure 9. *Saturation curves (deaths)*

Table 7

Parameters of the curves(deaths)

Param.	Wave1	Wave2	Wave3	Wave4
K	583.413	14920.64	31727.39	54383.18621
c	124.657	136986.1	31876.6436	487.3019
r	0.0987	0.0426	0.021227	0.010846167

Comparison of the saturation curves shows that the fourth wave had the highest number of cases (*K* parameters), but it was a little bit slower in case of number of deaths, possibly because of the effects of vaccination.

Effects of vaccination can be seen also by comparison of the derivatives of the saturation curves, seen in *Figures 10* and *11*. *Equation (10)* shows the equation of the derivative for infections, as a function of the days and the parameters of this equation are the same as in *Equation (1)*.

$$\frac{dy(x)}{dx} = \frac{Kcre^{-rx}}{(1+ce^{-rx})^2} \tag{10}$$

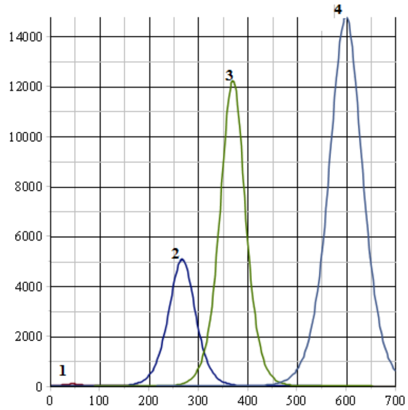

Figure 10. *Derivatives of the logistic curves of the waves (number of infections)*

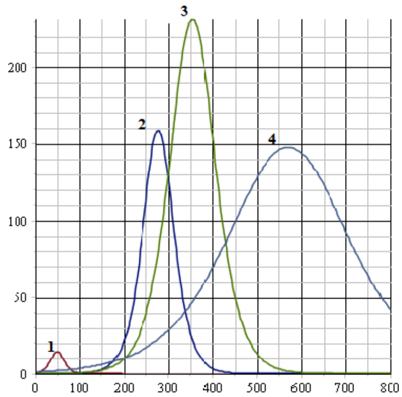

Figure 11. *Derivatives of the logistic curves of the waves (number of deaths)*

Comparing the derivative curves shown in *Figures 10* and *11*, it can be seen that the distance between the curve maximum points is smaller in the case of wave two and three, than in case of waves four and three, both for the number of infections and the number of deaths, too. The larger distance between the maximum points of the curves means a longer time before the new virus variant appears, so there was a longer “mutation delay”. This delay also can be because of the effects of the vaccination, since in Hungary at that time the number of vaccinations was relatively high, and the number of people who had recovered from the disease was also high, which means a lower number of active patients, therefore there was smaller “space” for the virus for the generation of the new variant.

5. Conclusions of the comparisons

It can be seen from the previous points that the sigmoid curves describing the time history of the waves of the coronavirus disease have two important parts. The first part is the exponential growth, which shows the free, unconstrained reproduction and infection process, which is true when people do nothing against the virus. In this period, regarding the number of infections: it is possible to see the real aggressiveness of the disease, the real “face” of the virus, its virulence, spreading speed, or its ability to reproduce. Investigating the number of deaths, in this starting period will indicate, how serious the disease is and how fatal the given virus variant is. The exponential growth of the waves for the number of infections is shown in *Figure 6*, where it can be concluded that the third wave is by far the most aggressive in terms of the number of infections and the fourth wave is close to it. The parameters shown in *Table 4* and *5* can help us compare the curves if they are very close each to another (waves 2, 4 and 1) and they show only small differences, which could be difficult to see at first look.

The exponential curves of the waves for the number of deaths due to the coronavirus are shown in *Figure 7*. In this case also the third wave is the most dominant, however the second wave also seems to be aggressive. Comparing the exponential curves, an important aspect to consider is how long the exponential part of the growth is, since longer exponential parts will considerably increase the numbers, which will mean a higher number of infections or higher number of deaths. The end of the exponential part is shown by the appearance of the inflexion point, when the disease enters the saturation part of the growth. From this point the number of new cases will decrease day by day until it is close to zero, which means the end of the wave. After the end of a wave, a new wave can be started if a new virus mutant is generated. The probability of the new mutation is high if the total number of infections was high during the total time of the wave, according to the "law of large numbers". Therefore the day of the inflexion point is a very important characteristic, and a simple means of comparison is the number of days elapsed from the beginning of the wave until the appearance of the inflexion point. It could be important to define the day of "starting" of the wave: at the end of a wave, small numbers of daily cases are present and if the new wave is ready to start, it will have increasing numbers, so the two waves will be present together at the same time. The day when the number of cases of the new wave is equal to the number of cases of the previous wave can be considered as the beginning day of the new wave. This is very easy to decide by comparing the values of the functions or comparing the shapes of the curves. *Table 7* shows the number of days elapsed until the inflexion point for the four waves.

Table 8

Days elapsed until the inflexion point

wave	number of nfections	number of deaths
1	50	40
2	75	100
3	116	120
4	167	180

If the inflexion point appears later, this shows the longer continuance of the disease, which could be caused by the aggressiveness of the variant, by the measures being put into effect later, or by less strength or efficiency of the measures against the disease.

The distance between the inflexion points of the adjacent waves could be also an important characteristic which can be easily described by numbers and easily compared numerically. This distance is in connection with the speed of the generation of the new mutation: a longer distance means a higher "mutation delay", while shorter distance shows the quick appearance of the new variant. *Table 9* shows this mutation delay distance for the investigated waves.

Comparison of the mutation delay numbers of the waves show that the new variant arrived most quickly after the second wave, and this variant caused the third wave. The causes of this very short mutation distance (approximately half as much as for the other waves) could be the higher number of total infections in second wave and the fact that the vaccination did not reach yet a high enough level for herd- immunity. After the third wave the mutation delay increased once more to a higher level, probably because of the positive effects of the higher vaccination rates, even though the total number of the cases was very high.

Table 9
Mutation delay of the waves

waves	number of infections	number of deaths
1–2	200	209
2–3	114	91
3–4	215	218

Further comparisons are possible investigating the second part of the growth process, the logistic curves of the waves. Maybe it was already obvious from the previous results, but comparing the logistic waves in *Figure 8* and *9* it can be seen very clearly that the first wave was very weak, almost negligible compared to the other waves, both in case of the number of infections and the number of deaths.

In the case of the logistic curves, the first parameter which is easy to compare, is the parameter *K*, showing the maximum number of the cases in the wave (saturation level of the numbers). *Figure 8* and *9*, in good agreement with *Table 6* and *7* show that the value of *K* increases with time, meaning that newer waves have higher values of maximum numbers of infections and deaths. This means that consecutive waves are more harmful, regarding both the number of infections and the number of deaths. Comparing the speed of the growth (parameter *r*) the conclusion is similar, with the only difference that the fourth wave has a slightly smaller *r* parameter, so slower growth speed (maybe because of increasing immunity from vaccination), but the total number of the cases is the highest amongst the waves.

Considering the derivative curves (*Figures 10* and *11*), the positions of the curves show the spectrum of the disease, each wave has its eigenvalue (the place of the inflexion point) and the amplitude (maximum value of the derivative). This spectrum is very similar to the spectrum of a vibrating system, therefore the ratio of the width at half maximum over the place of the maximum [Equation (7)] can be also an interesting characteristic parameter of the given wave. This parameter in the case of a vibrating system is related to damping and energy dissipation: in the case of the pandemic this parameter could be connected to the importance or significance of the given wave, which we can call the "significance factor" or "extent" factor. *Table 10* shows the extent factors of the waves.

Table 10
Extent factors of the waves

wave	infections	deaths
1	0.2	1.0
2	4.0	5.17
3	10.2	3.83
4	9.6	1.45

The extent factor can give information also for the runoff, or the long-drawn state of the wave, where a higher extent factor means a steep curve and short duration of the disease but a high number of cases, while higher extent factor shows longer duration and a lower maximum.

Comparing the amplitudes, from *Figure 10* it can be concluded that the amplitudes of the waves increase continuously as a function of time, and newer waves have higher amplitude than the previous waves. This shows that the disease is becoming more aggressive and it can cause a higher number of infections. This tendency is continuing even though vaccination is advancing, which demonstrates that the vaccination will not protect against the infection, but will make easier to recover. This conclusion is in agreement with *Figure 11*, where it can be seen that the maximum amplitude of wave four is considerably lower than the previous amplitudes, which can be in connection with the fact that wave four is in the time period where the rate of vaccination in the population of Hungary was high.

The last part of the history investigated here is from December 2021 until June 2023, which can be seen in *Figure 12* for number of infections and for number of deaths.

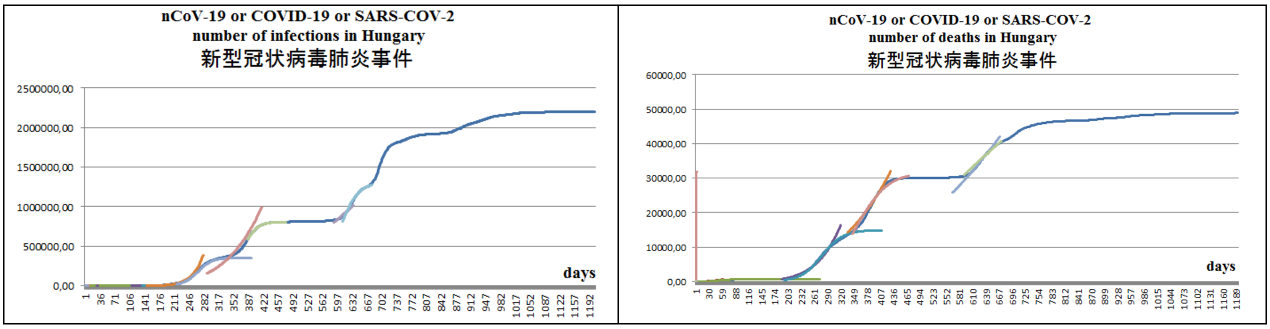

Figure 12. *History from December 2021 to June 2023*

From *Figure 12* it can be seen that wave five and six will finish with a long saturation period. This period contains relatively high number of infections, and smaller number of deaths, which may well demonstrate the effects of vaccination and mass immunity. Another tendency is that each new mutant virus variation caused a higher number of infections but their mortality rate was lower as a function of the time. In July 2023 the authorities ceased supplying data due to the very small number of deaths and small and decreasing number of infections. At the time of writing this paper (February 2024) the number of respiratory tract diseases is once again high because of several viruses, amongst them COVID-19. The exact numbers of infections and deaths are not available, but it is clear that the tendency of a high number of infections and smaller number of deaths is continuing. The situation could be very similar to the sixth wave (around day 850), so it is possible that the COVID-19 could be treated similarly to several other viruses of the respiratory tract that cause endemic disease from time to time.

6. Summary

In this paper the time history of six waves of COVID-19 in Hungary has been compared on the basis of sigmoid curves of the waves. Registering the real official data for the daily number of infections and deaths, the approximating sigmoid curves were built applying the least squares approximation method, solving it as an optimization problem searching for the minimum of the sum of the distances, using the Nelder-Mead unconstrained optimization algorithm.

During the comparisons the shape, trajectory of the curves, and the parameters in the equations of the curves has been studied. In the first part of the comparison the free growth (exponential curves) was investigated, which can show the severity of the virus variant in the starting period of the disease. The saturation period is described by logistic curves, compared in the second part of the comparison process.

Two important conclusions could be drawn. The first new result is the “mutation delay”, the time necessary for a new virus variant to appear in the population. In the case of higher number of infections, the probability of a mutation is higher, which will lead to a shorter mutation delay. This delay can be seen numerically and can be measured from the comparison of the derivatives of the curves (distance of maximums). A longer mutation delay could be also because of the effects of vaccination, which is in agreement with the fact that when the number of vaccinated people was high, this delay was longer (between waves three and four). Another result is discovering the similarity of the derivative curves to a spectrum of a vibrating system and finding that the eigenvalues of the waves can be identified. Around the eigenvalue, similarly to the damping factor of the vibrating system, the “extent” factor can be defined, which can show numerically the prolongation of the disease. This factor is easy to compare, in order to qualify and to range the severity of the waves.

The results and conclusions of the investigations presented in this paper could give interesting and useful information for the experts of the protection, epidemiologists and decision makers against the pandemic to predict the possible aggressiveness, growth speed of a wave, and the maximum possible number of infections and of deaths. On the basis of this information it would be easier or quicker to determine the necessary number of workers and beds in hospitals and the necessary quantity of equipment and medicaments. Understanding the behaviour of the curves and discovering the meaning and effects of the parameters of the curves and their derivatives can give very useful suggestions and new points of view for the investigation, comparison and qualification of other phenomena of our life, too:

The results achieved during this study could give useful information for example in product design during the investigations of product life curves, or for the comparison, qualification and analysis of several products, while for teachers it could be useful during comparison of the work of student groups. In the case of optimization algorithms, the study and comparisons of the iteration history curves of the algorithms can cut the time necessary for numerical experiments to find the better settings of the algorithm for a given example, therefore the results of this paper could give interesting and new points of view not only in case of diseases but in several other fields of our life too.

In some cases where the investigated curves are very similar, showing only very slight differences, it could be useful to apply the EBSYQ system (Evolutionary Based System for Qualification of Group Achievements). The table used in this system can show more precisely and accurately the differences and this will help in the comparison and qualification process. The investigation presented here can be done also for other human or animal diseases in order to discover the behaviour of viruses or predict the severity and aggressiveness of the disease. For this the availability of the appropriate data is indispensable.

Another very interesting and important possibility for the usage of these results could be to predict the behaviour of several phenomena which can be described by sigmoid curves. Building the curves by using some points in the starting phase of the growth of the phenomenon, the parameters and the curve shape could give the possibility for making even relatively long- term predictions.

7. Acknowledgement

The author of this paper would like to express his respect and appreciation to all experts, doctors, nurses and health workers contributing to the health and recovery of people infected during the COVID-19 pandemic and during the vaccination process, and for their efforts exerted in order to confine or conquer the disease. “May success crown” their efforts against the coronavirus COVID-19!

References

[1] Abd Al-Rahman, N. E. (2022). Abu-Hussien, A. E., Yehia, E. G., Mousa, S. A.: Modeling Sigmoidal Growth Curves to Study the Confirmed Cases of COVID-19 in Egypt. *Academy of Business Journal, Al-Azhar University*, Vol 27, January, 23 p.

[2] Anilkumar, B., Srividya, K., Sowjanya, M. A. (2023). COVID-19 classification using sigmoid based hyper-parameter modified DNN for CT scans and chest X-rays. *Multimed Tools Appl.*, 82 (8), pp. 12513–12536 PMCID: PMC9485800 , PMID: 36157352

[3] Bertalanffy, L. (1960). Principles of Theory of Growth. In: *Fundamental Aspects of Normal and Malignaent Growth*. Amsterdam. pp. 137–259.

[4] CDC COVID-19 Response Team: Severe Outcomes Among Patients with Coronavirus Disease 2019 (COVID-19) in United States, February 12 – March 16, 2020. *Morbidity and Mortality Weekly Report*, 12, pp. 343–346. **https://doi.org/10.15585/mmwr.mm6912e2**

[5] Dénes, A., Ibrahim, M.A., Oluoch, L. et al. (2019). Impact of weather seasonality and sexual transmission on the spread of Zika fever. *Sci. Rep.*, 9, p. 17055. **https://doi.org/10.1038/s41598-019-53062-z**

[6] Dubey, R. S., Mishra, M. N, Goswami, P. (2022). Effect of COVID-19 in India – A prediction through matematical modeling using Atangana Baleanu fractional derivative. *Journal of Interdisciplinary Mathematics*, Vol.25, Issue 8. pp 2431–2444. **https://doi.org/10.1080/09720502.2021.1978682**

[7] Du, Z., Xu, X., Wu, Y., Wang, I., Cowling, B. J., Meyers, L. (2020). Serial Interval of COVID-19 among Publicly Reported Confirmed Cases. *Emerging Infectious Diseases*, 6, pp. 1341–1343. **https://doi.org/10.3201/eid2606.200357**

[8] Fisher, J. C., Pry, R. H. (1971). A Simple Substitution Model of Technological Change, *Technological Forecasting and Social Change*, 3. pp. 75–88.

[9] Gruener, S. (2024). Determinants of Gullibility to Misinformation: A Study of Climate Change, COVID-19 and Artificial Intelligence. *Journal of Interdisciplinary Economics*, Vol 36, Issue 1, pp. 58–78. **https://doi.org/10.1177/02601079221083482**

[10] Jang, S.L., Dai, S. C., Sung, S. (2005). The pattern and Externality Effect of Diffusion of Mobile Telecommunications: the Case of OECD and Taiwan. *Information Economics and Policy*, 17, pp. 133–148.

[11] Johns Hopkins University homepage (2023). COVID-19 Dashboard by the Center for Systems Science and Engineering (CSSE) at Johns Hopkins University (JHU). https://gisanddata.maps.arcgis.com/apps/opsdashboard/index.html#/bda7594740fd40299423467b48e9ecf6, last visit: 18 July, 2023.

[12] Kapoor, S., Amand, V., Arya, A., Kumar, A. (2023). Two Years of COVID-19, Analysis of Global India's Pandemic Response, *Journal of Public Health and Primary Care*. **https://doi.org/10.4103/jphpc.jphpc_4_23**

[13] Konstantinov, M., Konstantinov, K., Konstantinov, S. (2021). Sigmoid models for COVID-19 pandemic. *AIP Conf. Proc.*, 2333, 090002, Vol 2333, Issue 1, 8 March 2021. **https://doi.org/10.1063/5.0041728**

[14] Kozuko, F., Bajzer, Z. (2003). Combining Gompertzian Growth and Cell Population Dynamics, *Mathematical Biosciences*, 185, pp. 153–167.

[15] Lennert, J. (2021). The spread of SARS-COV-2 virus in Hungary – agent-based modelling scenarios for the first wave of the pandemic (in Hungarian), *Tér és Társadalom*, Vol. 35, No. 3, 32 p. **https://doi.org/10.17649/TET.35.3.3341**

[16] Lorentz, M. O. (1905). Methods of Measuring the Concentration of Wealth. *Publications of the American Statistical Association*, Vol. 9, No. 70, pp. 209–219.

[17] Malthus,T. (1798). *An Essay on the Principle of Population.* Printed for J. Johnson in St Paul's Church-Yard, London, 1798.

[18] Mansfield, E. (1961). Technical Change and the Rate of Imitation. *Econometrica*, Vol. 29, No. 4, pp. 741–766. October.
[19] Meyer, W. B., Turner, B. L. (eds.) (1994). *Changes in land use and land cover: a global perspective*. Cambridge University Press, p. 537.
[20] Mitscherlich, E. A. (1909). The law of minimum and the law of diminishing soil productivity. (In German). *Landwirtshaftliche Jahrsbücher*, 38, pp. 537–552.
[21] Moore, E. G. (1965). Cramming more Components onto Integrated Circuits. *Electronics Magazine*, 38 (8), pp. 114–117.
[22] Mousa, S. A. et al. (2023). Proposed Double Sigmoidal Growth Curves: Modeling and Estimation. *Calcified Tissue International*, January. **https://doi.org./10.21608/alat.2023.280932**
[23] Nelder, J. A., Mead, R. (1965). A simple method for function minimisation. *Computer Journal* 7. pp 308–313. **https://doi.org/10.1093/comjnl/7.4.308**
[24] Nikosz, F. (2020). Növekedési görbék, társadalmi diffúzió, társadalmi változás. (in Hungarian, Growth curves, social diffusion, social changing) http://www.socialnetwork.hu/cikkek/Fokasz Diffuzio.pdf, last visit: 10 Oct. 2020, *Szociológiai Szemle*, 2006/3, pp. 19–51.
[25] Novoa-Munoz, F. (2022). Models to Predict the Number of Infected Cases and Death from COVID-19 in Chile and its Most Affected Regions. *Hindawi Discrete Dynamics in Nature and Society*, Vol. 2022, ID 1906435. **https://doi.org/10.1155/2022/1906435**
[26] Pearl, R.; Reed, L. J. (1920). On the Rate of Growth of the Population of the United States since 1790 and its Mathematical Representation. *Proc. of the National Academy of Sciences*, Vol. 6, No 6, pp. 275–288.
[27] Rézsó, F.-né (2020). Szigmoid görbék alkalmazása tanulói csoportok eredményeinek vizsgálatához. (In Hungarian, Application of sigmoid curves for the investigations of student groups) *Multidiszciplináris tudományok*, 10. kötet, 3 sz., pp. 195–211. **https://doi.org/10.35925/j.multi.2020.3.25**
[28] Richards, F. J. (1959). Flexible Growth Function for Empirical Use. *Journal of Experimental Botany*, 10, pp. 290–300. **http://dx.doi.org/10.1093/jxb/10.2.290**
[29] Shen, C. Y.: Logistic growth modelling of COVID-19 proliferation in China and its International implications. *International Journal of Infectious Diseases*, 96, pp. 582–589.
[30] Somathilake, L. W. (2022). A mathematical model for control strategies of COVID-19. *Journal of Interdisciplinary Mathematics*, Vol. 25, Issue 8, pp 2365–2386. **https://doi.org/10.1080/09720502.2021.1959002**
[31] Somefun, O. A., Akingbade, K. F., Dahunsí, F. M. (2020). From the logistic-sigmoid to nlogistic-sigmoid: Modeling the COVID-19 pandemic growth. *arXiv:*2008.04210, 9 Dec. 2020, v3, 11 pages. **https://doi.org/10.48550/arXiv.2008.04210**
[32] Szabó, F. J. (2011). Analógia a sport- világcsúcsok története és az evolúciós optimáló algoritmusok iteráció- története között. (in Hungarian). Analogy of history of sports world records and iteration history of evolutionary optimization algorithms. *GÉP*, LXII; pp. 9–10., pp. 28–31., 4 p.
[33] Szabó, F. J. (2017). Evolutionary Based System for Qualification and Evaluation of Group Achievements (EBSYQ). *International Journal of Current Research*, Vol. 9, Issue 08, pp. 55507–55516, August, 2017.
[34] Szabó, F. J. (2018). Optimumkereső algoritmusok iterációtörténetének vizsgálata. (in Hungarian, Investigation of iteration history curves of optimization algorithms) *GÉP*, 69, (4), pp. 82–85.
[35] Szabó, F. J. (2019). Application of sigmoid curves in environmental protection. In: Szita Tóthné, Klára, Jármai Károly, Voith Katalin (eds.). *Solutions for Sustainable Development: Proceedings*

of the 1st International Conference on Engineering Solutions for Sustainable Development, (ICESSD 2019). London, United Kingdom: CRC Press, pp. 1–7, 7 p.
[36] Szabó, F. J. (2020). A COVID-19 járvány időbeli alakulásának vizsgálata szigmoid görbékkel. (in Hungarian, Study of COVID-19 history by sigmoid curves) *Multidiszciplináris Tudományok*, 10, 3, pp 294–306, 13 p. **https://doi.org/10.35925/j.multi.2020.3.35**
[37] Szabó, F. J. (2021). Analysis of Wear Curves as Sigmoid Functions. *Lecture Notes in Mechanical Engineering*, 22, pp 273–281, 14 p. **https://doi.org/10.1007/178-981-15-9529-5_24**
[38] Szabó, F. J. (2021). A szigmoid görbék multidiszciplinaritása. *GÉP*, LXXII, 3–4, pp 61–64, 4 p (in Hungarian, multidisciplinarity of sigmoid curves).
[39] Szabó, F. J. (2022). Time history of COVID-19 pandemic by sigmoid curves II. (in Hungarian). *Multidiszciplináris Tudományok*, Vol. 12, No. 1, pp. 58–70. **https://doi.org/10.35925/j.multi.2022.1.5**
[40] Törnquist, L. (1981). Collected scientific papers of Leo Törnquist. *Research Institute of the Finnish Economy*. Series A.
[41] Verhulst, P.- F. (1847). Deuxieme mémoire sur la loi d'accroissement de la population. Mémoires de l'Académie Royale des Sciences, des Lettres et des Beaux- Arts de Belgique. 20, 32, p. 1847, Retrieved 18 February 2013.